A Suppression method of Discharge Current Oscillations in a Hall Thruster

Naoji Yamamoto[1], Kimiya Komurasaki[2] and Yoshihiro Arakawa[3]
[1]Department of Advanced Energy Engineering Science, Kyushu University
6-1 Kasuga-kouen, Kasuga, Fukuoka 816-8580, Japan
[2, 3] Department of Aeronautics and Astronautics, University of Tokyo
Hongo 7-3-1, Bunkyo-ku, Tokyo, 113-8656, Japan
+81-3-5841-6586

Discharge current oscillation at frequency range of 10-100kHz in Hall thrusters was investigated for extending the stable operational range of them. An oscillation characteristic was measured using a 1kW class Hall thruster. An oscillation model was proposed based on experimental results. The predicted frequency and unstable operational condition agreed qualitatively with the experimental results. This model shows that acceleration channel configuration will affect the stability, and experimental results validated this recipe.

Nomenclature

B	: magnetic flux density
D	: diffusion coefficient
E	: electric field strength
e	: electronic charge
I_d	: discharge current
I_{sp}	: specific impulse
k	: wave number
k_B	: Boltzmann's constant
L	: ionization zone length
m	: particle mass
$\dot{m}$	: mass flow rate
N	: number density
r_L	: Larmor radius
S	: cross-section
T	: temperature
V	: volume
V_e	: electron velocity
V_n	: neutral atom velocity
V_d	: discharge voltage
z	: axial direction
Δ	: oscillation amplitude
η_a	: acceleration efficiency
λ_{ne}	: neutral-electron mean free path
μ	: mobility
σ_{di}	: atom ionization collision cross section
σ_T	: atom total collision cross section
τ	: measurement time
ϕ	: diameter
ω	: oscillation frequency

Subscripts

B	:	Bohm diffusion
c	:	classical diffusion
e	:	electron
i	:	ion
n	:	neutral atom
out	:	outer
r	:	radial direction
0	:	anode side
1	:	exit side

Introduction

There are various types of Hall thruster, and they could be nearly categorized into two types; magnetic layer type and anode layer type. [1, 2] One of the former type Hall thrusters is "Stationary Plasma Thruster" (SPT), which has been developed in Russia. [3, 4] The distinguish features of this type are continuous and extended acceleration zone for the sufficient ionization and the stability. On the other hand, "Thruster with Anode Layer"(TAL), having been developed in Russia as well, [5, 6] is categorized into the later type. The feature of this is narrow acceleration zone for the reducing the loss of ion and electron collisions with walls. [7, 8]

One of the problems in Hall thrusters is about discharge current oscillation, especially at frequency range of 10-100 kHz. It may cause the operation to cease, and may bear down on Power Processing Unit (PPU) as well. Understanding the oscillation is essential for future improvement of Hall thrusters, especially of anode layer type. There have been many studies about this oscillation phenomenon, and they revealed that this oscillation would be caused by ionization instability.[9-11] They, however, were not enough to adequately describe this oscillation, especially stability criteria for a certain range of magnetic flux density. The aim of this study is 1) to propose a physical model related to the oscillation 2) to validate the model by comparing analytical and experimental results and 3) to extend stable operational condition range.

---

[1] Research Associate, Member AIAA
[2] Associate Professor, Member AIAA
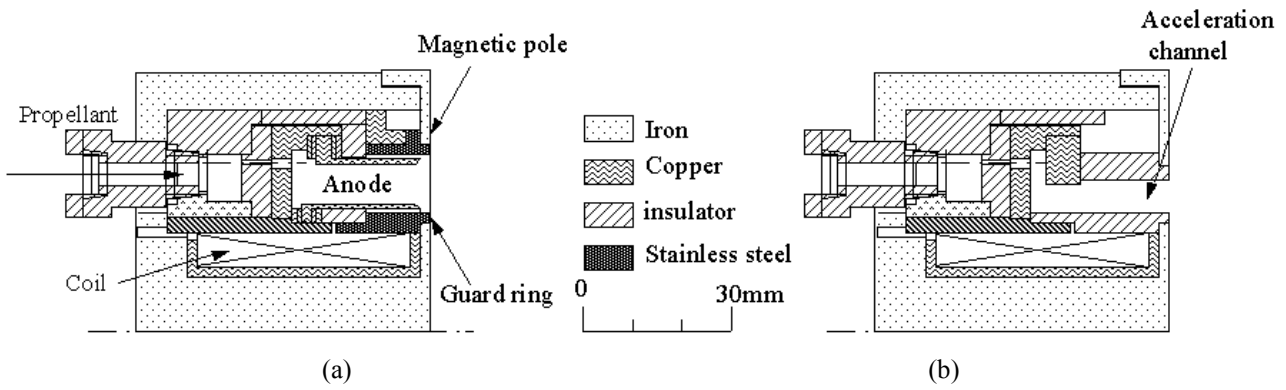[3] Professor, Member AIAA

Fig. 1 Cross section of the Hall Thruster developed at University of Tokyo.
(a) anode layer type   (b) magnetic layer type

The Experimental Equipment

Thruster

Figure 1(a) shows the cross-section of a 1kW class anode layer type Hall thruster. The inner and outer diameter of the acceleration channel is 48 mm and 72 mm, respectively. The outer diameter can be changed to 62mm. A solenoidal coil is set at the center of the thruster to apply radial magnetic field in the acceleration channel. The magnetic flux density is variable by changing the coil current. There is no outer coil because of the keeping uniform magnetic field distribution along the azimuthal direction. The magnetic field distribution along the channel median is almost uniform in the short acceleration channel. Magnetic flux density is maximized on the inner wall and is decreased with radius since a magnetic flux is constant. In this study, thus, magnetic flux density at the channel median is taken as the representative value of magnetic flux density. Guard rings are made of stainless steel (SUS304). The separation between the guard ring and the anode is 1mm. It has a hollow annular anode, which consists of two cylindrical rings and a propellant gas is fed through them. The position and the width of the hollow anode are variable by changing the anode components. In this study, the width of the hollow anode is 3mm and the gap between the tip of the anode and the exit of the acceleration channel is fixed at 3 mm.

It can be Magnetic layer type Hall thruster if the acceleration channel wall made of BN was used as shown in Fig.1 (b). The inner and outer diameter of the acceleration channel is 48 mm and 62 mm, respectively. The anode is located at 21 mm upstream end of the acceleration channel.

Xenon gas was used as the propellant. As electron source, a fresh filament cathode (ϕ 0.27 mm×400 mm×3, 2 % thoriated tungsten) was used, since an aged hollow cathode in itself can be a noise source. A thrust was measured by a pendulum type thrust stand.[12] The error of the thrust measurement could be kept less than 2 mN. An ion beam current was measured by the ion beam collector that was located at 250 mm downstream of the thruster.

Vacuum Chamber

A 2m-diameter by 3m long vacuum chamber was used through the experiments. The pumping system consists of a diffusion pump, a mechanical booster pump and two rotary pumps. The background pressure was maintained under 5.3×10^{-3} Pa for most of the operating conditions.

Results and Discussion

Oscillation Characteristics

The amplitude of the oscillation would be a good indicator of stability since the operation can be stopped by oscillation. To evaluate the oscillation depth of the experimental results, the amplitude of oscillation, Δ, is defined as,

$$\Delta = \frac{\text{R.M.S}}{\overline{I_d}} = \frac{1}{\overline{I_d}}\sqrt{\frac{\int_0^\tau (I_d - \overline{I_d})^2 \, dt}{\tau}}, \quad (\overline{I_d} = \frac{\int_0^\tau I_d \, dt}{\tau}) \qquad (1)$$

Figure 3 shows the relation between the thrust performance and the magnetic flux density. The oscillation amplitude was changed sensitively with B. The stable operation can be seen at very narrow range near the $B \approx 0.016$ T or $B > 27$ mT in this configurations, though the thrust efficiency was low on the condition of $B > 27$ mT. This is because the discharge current was suddenly increased beyond $B = 27$ mT. Thus, the suitable operational range was narrow and thence extending stable operational range was need. This sensitivity characteristic to B will show that electron mobility would affect this oscillation rather than ion mobility would.

In addition, the transition of an operational regime at $B = 27$ mT will be caused by the transition of electron diffusion from the classical diffusion to the anomalous diffusion. That is, an electron moves to the anode with the classical diffusion on the condition of $B < 27$ mT, and it does with the anomalous diffusion on the condition of $B > 27$ mT as shown in Fig.4. It was interesting phenomenon that the oscillation regime was also changed at this point. This was another mark that electron mobility would affect this oscillation.
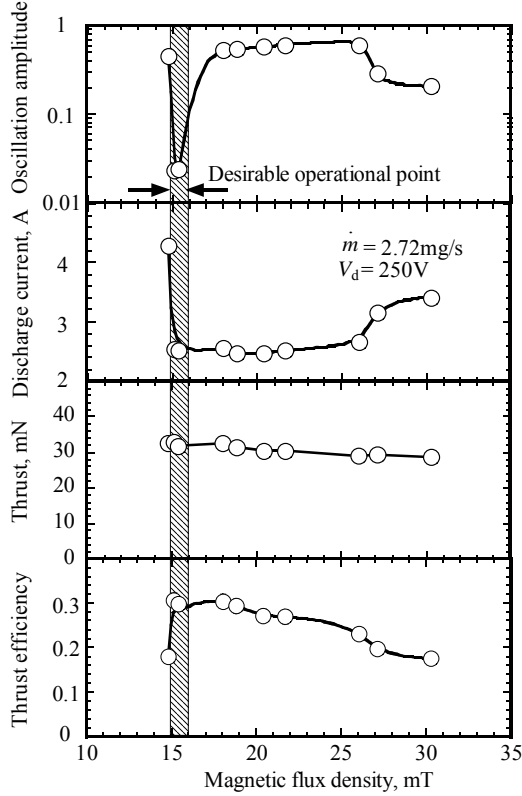
Fig. 2 Oscillation characteristics.
ϕ_{out} =72 mm, $\dot{m}$ =2.72 mg/s, V_d=250 V

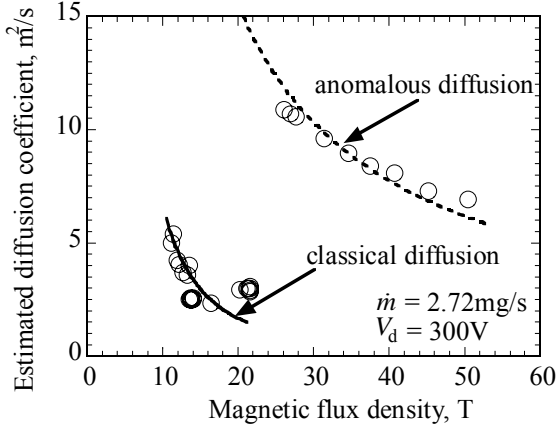Fig. 3 Estimated electron diffusion coefficient.
ϕ_{out} =72 mm, $\dot{m}$ = 2.72 mg/s, V_d= 300 V

Oscillation Model

Several studies indicated that this oscillation was caused by ionization instability,[9,13] that is, the disturbance of neutral atom number density cause the disturbance of plasma density, and it feeds back to the disturbance of neutral atom density.

Baranov's model,[9, 14] however, was not enough to adequately describe this oscillation, especially stability criteria for a certain range of magnetic flux density. Thus, revised ionization instability model was proposed.

The set of equations describing this oscillation are below two equations, equation of continuity for neutral atom and for electron. The continuity for ion was not adopted,[10] since the diffusion rate of plasma is controlled by the slower species and that is electron in Hall thrusters, for electron was trapped by the magnetic filed. The equation of continuity for neutral atom

$$\int_V \frac{\partial N_n}{\partial t} dV + \int_S N_n V_n dS = \int_V -\langle \sigma_{di} v_e \rangle_{T_e} N_n N_e dV \cdot \quad (2)$$

The equation of continuity for electron

$$\int_V \frac{\partial N_e}{\partial t} dV + \int_S N_e V_e dS = \int_V \langle \sigma_{di} v_e \rangle_{T_e} N_n N_e dV. \quad (3)$$

To solve these equations analytically, linearization was done. The phase velocity of perturbation of neutral atoms was propagated as its axial velocity. On the other hands, the phase velocity of perturbation of plasma is assumed as zero, since plasma in the ionization zone will fluctuate monolithically.[15] This is a unique point of this model, because the relaxation time of plasma $(\approx (L/\pi)^2/2D \approx 0.2\ \mu s)$ is less than oscillation period (≈ 30 μs), though Baranov assumed that perturbation of plasma would propagated as the same phase velocity of disturbance of neutral atoms.[14]

$$N_n = N_n + n_n \exp[-i\,(\omega\,t - k_n z)] \quad (4)$$

$$N_e = N_e + n_e \exp[-i\omega\,t]\cdot \quad (5)$$

where, $k_n = C_n + i\,1/\lambda_{ne}$, $C_n \approx \mathrm{Re}[\omega]/2\pi V_n$.

For the simplicity, $\langle \sigma_{di} v_e \rangle_{T_e}, N_n, N_e$ is considered as $\overline{\langle \sigma_{di} v_e \rangle_{T_e}}, \overline{N}_n, \overline{N}_e$ and boundary condition is defined as shown in as Fig. 4.

$$\overline{\langle \sigma_{di} v_e \rangle_{T_e}} = \frac{1}{L}\int_0^L \langle \sigma_{di} v_e \rangle_{T_e}\ dz,$$

$$\overline{N}_n = \frac{1}{L}\int_0^L N_n\ dz, \quad (6)$$

$$\overline{N}_e = \frac{1}{L}\int_0^L N_e\ dz,$$

If electron moves to the anode with the classical diffusion, electron velocity is assumed to oscillate since electron velocity is proportional to neutral atom density. Electron velocity is written as below.

$$V_e = V_e + v_e$$
$$= -\frac{m_e <\sigma_T v_e>_{en}}{eB^2}(E + \frac{k_B T_e}{e}\frac{\nabla N_e}{N_e})(N_n + n_n) \quad (7)$$
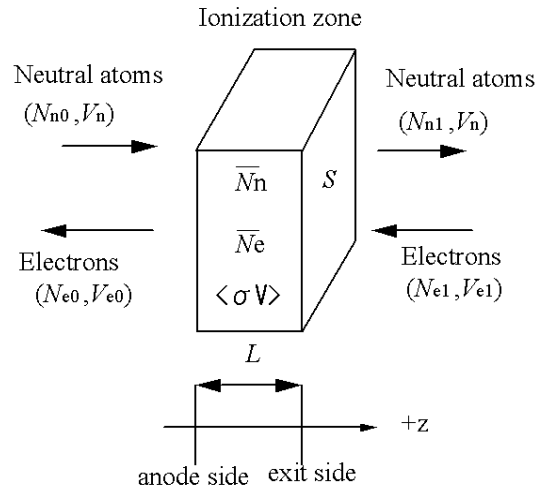$$\equiv f(z)\,(N_n + n_n).$$

Fig. 4 Schematic of ionization zone in this model.

Substituting Eqs. (5) and (6) into Eq. (4), the dispersion relation is written as,

$$\omega^2 + \left\{ i \overline{\langle \sigma_{di} v_e \rangle}_{T_e} (\overline{N}_e - \overline{N}_n) + i \frac{V_{e1} - r_S V_{e0}}{L} - GV_n \right\}\omega$$
$$+ iG\left(\overline{\langle \sigma_{di} v_e \rangle}_{T_e} \overline{N}_n V_n - \frac{V_{e1} - r_S V_{e0}}{L} V_n + \overline{\langle \sigma_{di} v_e \rangle}_{T_e} \overline{N}_n f_1 N_{e1} \right) \quad (8)$$
$$- \overline{\langle \sigma_{di} v_e \rangle}_{T_e} \overline{N}_e \frac{V_{e1} - r_S V_{e0}}{L} = 0$$

where $G = \dfrac{k_n \times \exp[ik_n L]}{\exp[ik_n L] - 1}, \qquad r_S = \dfrac{S_0}{S_1}.$

Solving above dispersion relation, the frequency of this oscillation, Re [ω] is written as,

$$f_c = \frac{1}{2\pi} \mathrm{Re}[\omega] = \frac{1}{2\pi}(\frac{1}{2}(-a_c + \mathrm{Re}[\sqrt{(a_c + ib_c)^2 - 4(c_c + id_c)}]) \quad (9)$$

The stability condition of this oscillation, Im [ω]<0 is written as,

$$b_c > 0 \qquad (10)$$
$$b_c^2 c_c - a_c b_c d_c + d_c^2 < 0 \qquad (11)$$

Where

$a_c = -\mathrm{Re}[G] \times V_n$

$b_c = \dfrac{V_{e1} - r_S V_{e0}}{L} - \overline{\langle \sigma_{di} v_e \rangle}_{T_e} \overline{N}_n + \overline{\langle \sigma_{di} v_e \rangle}_{T_e} \overline{N}_e - \mathrm{Im}[G] \times V_n$

$c_c = -\mathrm{Im}[G] \times \left(\overline{\langle \sigma_{di} v_e \rangle}_{T_e} \overline{N}_n V_n - \dfrac{V_{e1} - r_S V_{e0}}{L} V_n + \overline{\langle \sigma_{di} v_e \rangle}_{T_e} N_n f_1 N_{e1} \right)$

$\qquad - \overline{\langle \sigma_{di} v_e \rangle}_{T_e} \overline{N}_e \dfrac{V_{e1} - r_S V_{e0}}{L}$

$d_c = \mathrm{Re}[G] \times \left(\overline{\langle \sigma_{di} v_e \rangle}_{T_e} \overline{N}_n V_n - \dfrac{V_{e1} - r_S V_{e0}}{L} V_n + \overline{\langle \sigma_{di} v_e \rangle}_{T_e} N_n f_1 N_{e1} \right)$

If electron moves to the anode with the Bohm diffusion, electron velocity is written as

$$V_e = -\mu E - D\frac{\nabla n_e}{n_e} = -\frac{1}{16B}(E + \frac{kT_e}{e}\frac{\nabla n_e}{n_e}) \quad (12)$$

Thus, the dispersion relation is written as

$$\omega^2 + \left\{ -i \overline{\langle \sigma_{di} v_e \rangle}_{T_e} \overline{N}_n + i \frac{V_{e1} - r_S V_{e0}}{L} + i \overline{\langle \sigma_{di} v_e \rangle}_{T_e} \overline{N}_e - GV_n \right\}\omega \quad (13)$$
$$+ iGV_n\left(\overline{\langle \sigma_{di} v_e \rangle}_{T_e} \overline{N}_n - \frac{V_{e0} - r_S V_{e1}}{L} \right) - \overline{\langle \sigma_{di} v_e \rangle}_{T_e} \overline{N}_e \frac{V_{e1} - r_S V_{e0}}{L} = 0$$

The frequency of this oscillation Re[ω] is written as,

$$f_B = \frac{1}{2\pi} \mathrm{Re}[\omega] = \frac{1}{2\pi}(\frac{1}{2}(-a_B + \mathrm{Re}[\sqrt{(a_B + ib_B)^2 - 4(c_B + id_B)}]) \quad (14)$$

The stability condition of this oscillation Im [ω]<0 is written as,

$$b_B > 0 \qquad (15)$$
$$b_B^2 c_B - a_B b_B d_B + d_B^2 < 0 \qquad (16)$$

where

$a_B = -\mathrm{Re}[G] \times V_n$

$b_B = \dfrac{V_{e1} - r_S V_{e0}}{L} - \overline{\langle \sigma_{di} v_e \rangle}_{T_e} \overline{N}_n + \overline{\langle \sigma_{di} v_e \rangle}_{T_e} \overline{N}_e - \mathrm{Im}[G] \times V_n$

$c_B = -\mathrm{Im}[G] \times \left(\overline{\langle \sigma_{di} v_e \rangle}_{T_e} \overline{N}_n V_n - \dfrac{V_{e1} - r_S V_{e0}}{L} V_n \right) - \overline{\langle \sigma_{di} v_e \rangle}_{T_e} \overline{N}_e \dfrac{V_{e1} - r_S V_{e0}}{L}$

$d_B = \mathrm{Re}[G] \times \left(\overline{\langle \sigma_{di} v_e \rangle}_{T_e} \overline{N}_n V_n - \dfrac{V_{e1} - r_S V_{e0}}{L} V_n \right)$

Figure 5 shows the measured oscillation frequency and the predicted one. In the anode layer type, the predicted one was got from Eq. (9) since electron moves to anode with the classical diffusion. On the other hands, in the magnetic layer type, that was predicted from Eq.14 owing to the Bohm diffusion. The frequency of this

model agreed qualitatively with the measurement one. That is, both these frequencies were increased with discharge voltage. This tendency can be explained as below. To simplify equation (9) or (14), oscillation frequency could be rewritten as

$$f \approx \sqrt{\overline{\langle \sigma_{di} v_e \rangle}_{T_e} \overline{N}_e \frac{V_{e1} - r_S V_{e0}}{L}} \quad (17)$$

This equation shows that oscillation frequency will be increased with electron temperature. Thus, oscillation frequency will be increased with discharge voltage, since electron temperature will increase with discharge voltage. This also shows the reason why the frequency of the anode layer type was higher than that of the magnetic layer type. This is because the electron temperature of the anode layer type will be higher than that of the magnetic layer type,[2] and as experimental results did.
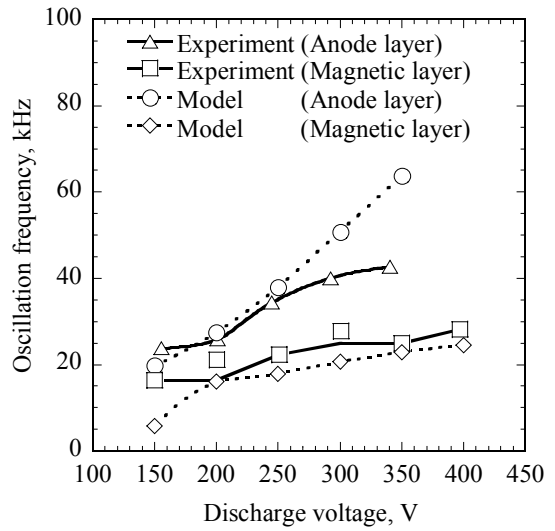

Fig. 5 Relation between oscillation frequency and discharge voltage.
anode layer type, ϕ_{out} =72 mm, $\dot{m}$ = 2.04 mg/s, B_r= 16 mT
magnetic layer type A, $\dot{m}$ = 1.36 mg/s, B_r= 14 mT

Figure 6 and 7 shows the measured oscillation amplitude and predicted stable/unstable operational condition. The hatched area indicates predicted stable operational condition deduced from this model and the doted area does that one deduced from Baranov's model.[14] There is a blank area, which indicate no data at the condition.

Experimental results showed that the stable operational range of B increase with $\dot{m}$. In addition, there were stable operation on the low magnetic flux density though η_a [16] is low. [17]

This model predicted that B with stable operation was increased with $\dot{m}$. It also predicted that there was unstable operation range between the stable operation ranges. Thus, It agreed with the experimental results in tendency, though it did not agreed quantitatively.

On the other hands, stable condition on the Baranov's model is

$$(\frac{\partial D_e}{\partial x} - V_n)^2 > \frac{(N_n - N_e)^2}{N_n} D_e \langle \sigma_{di} v_e \rangle_{T_e}. \quad (18)$$

Eq. (18) can be rewritten as " $\dot{m}$ <const - B^{-3} " and " $\dot{m}$ <B^{-3} ".[14] That is, the stable operational range of B was decreased with $\dot{m}$. Thus, It will not adequately describe this oscillation.

In the magnetic layer type, as well, this model adequately described stable range of this oscillation. Hence, this model would be a good expression of this oscillation mechanism. On the other hands, the stable condition on the Baranov's model are " $\dot{m} < B^{\alpha} (1 < \alpha < 1.5)$ "and " $\dot{m} < B^{-3}$ ".[14] It cannot predict the stable operation at the low magnetic flux density.

Examining this model with simplicity, the stable operational condition can be rewritten as

$$S_1 V_{e1} - S_0 V_{e0} - \bar{\gamma} \overline{N}_n SL > 0. \qquad (19)$$

This terms means the momentum transfer via the perturbation of plasma, i.e., viscosity effects. Thus oscillation was decayed if the viscosity coefficient, the left hand side of Eq.19, is negative.

In addition, this model shows the reason why the stable operation of the anode layer is narrower than that of the magnetic layer. This would be derived from the following reasons.

1. Electrons move to anode with the classical diffusion in the anode layer type. Thus as shown in Eq.(19), stable operation in the anode layer type is more sensitive than in the magnetic layer type.
2. Electron temperature of the anode layer type will be higher than that of the magnetic layer type. Thus, the left hand side of Eq. (19) in the anode layer type can be negative easier than in the magnetic layer type.
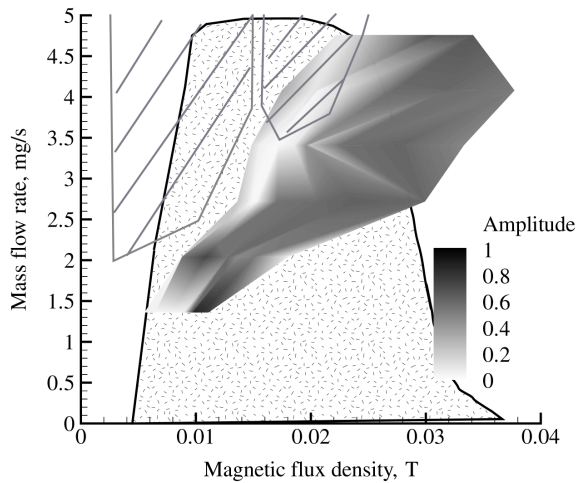

Fig. 6 Stable/unstable operational condition map. anode layer type, V_d=250 V.
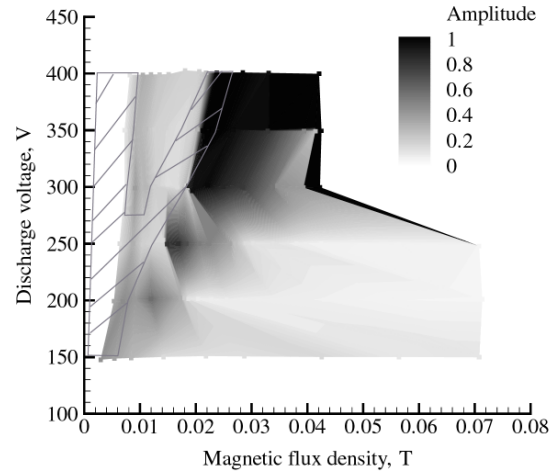

Fig. 7 Stable/unstable operational condition map. magnetic layer type, $\dot{m}$ =1.36 mg/s

Reduce the oscillation amplitude

Eq. (19) shows that increase in $S_0 V_{e0} / S_1 V_{e1}$ will make operation stable. Thus, oscillation amplitude was measured for various guard rings as shown in Fig. 8. The inner and outer diameter of the guard rings is 46mm and 64mm, respectively at the divergent type. The outer diameter is 60mm at the convergent type. Figure 9 shows the measured oscillation amplitude for various guard rings. Stable operational range of the convergent type was the largest among three, and that of the divergent type was the narrowest of all as this model showed. In addition, the propellant utilization of the convergent type was largest among them as shown in Fig. 10.

This model also shows that in a magnetic layer type, the adoption of convergent acceleration channel will also extend stable operation condition. The oscillation amplitude was measured for various acceleration channel configurations as shown in Fig. 11. The inner and outer diameter of the acceleration channel is 48mm and 52mm, respectively at divergent type. The outer diameter is 72mm at convergent type. The divergent type cannot keep discharge. Figure 12 shows the operational condition map with convergent acceleration channels. The stable operational range of convergent type is larger than that of parallel type as shown in Fig. 7. Thus, extending the stable operational condition range was succeeded.
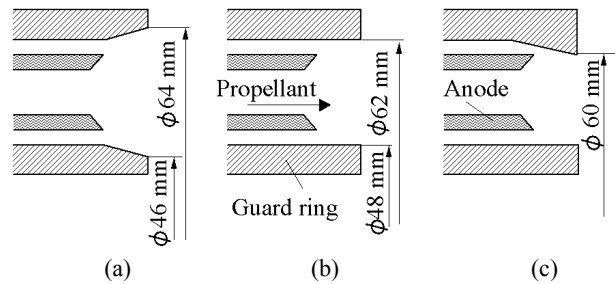

(a)   (b)   (c)

Fig. 8 Picture of various guard rings
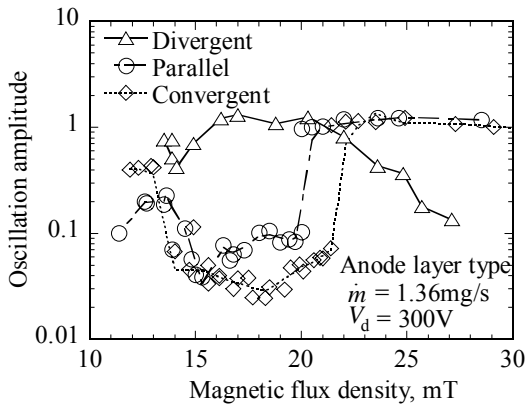(a) divergent (b) parallel (c) convergent

Fig. 9 Oscillation amplitude for various guard rings
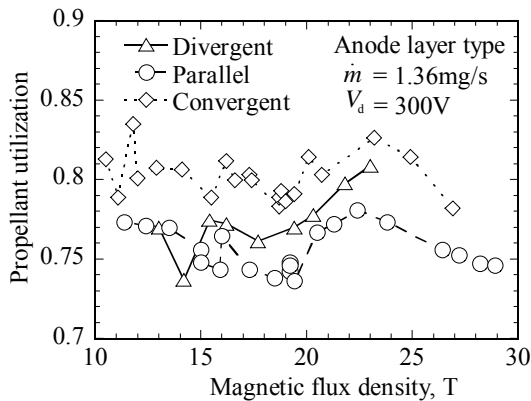

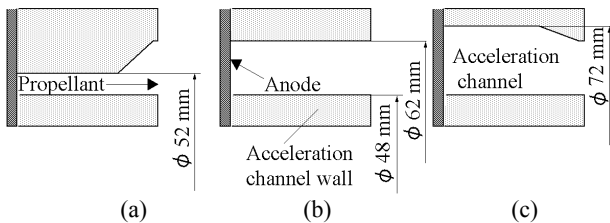Fig. 10 Propellant utilization for various guard rings

Fig. 11 Picture of various acceleration channels
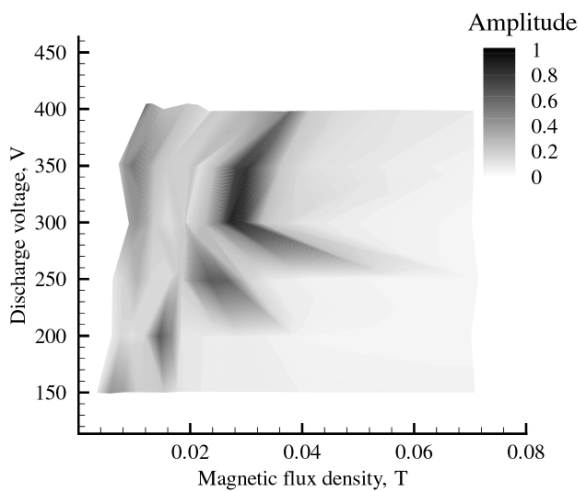(a) divergent (b) parallel (c) convergent

Fig. 12 Operational condition map with convergent
acceleration channel

Summary

An oscillation characteristic at frequency range of 10-100kHz was measured using a 1kW class Hall thruster. The oscillation amplitude was sensitive with magnetic flux density. Experimental results will indicate that electron mobility will affect this oscillation, thus, an oscillation model considering electron dynamics was proposed. This model could interpret measurement oscillation characteristics, the relation between oscillation frequency and discharge voltage or the relation between oscillation amplitude and magnetic flux density. This model also showed the origin of the difference of oscillation characteristics between the magnetic layer type and the anode layer type. This model proposed that a convergent acceleration channel configuration would reduce the oscillation amplitude and experimental results vindicated this recipe.

References

1 Kaufman, H. R., "Technology of Closed-Drift Thrusters," *AIAA journal*, 23, 1, 1985, pp.78-86.
2 Choueiri, E. Y.: Fundamental difference between the two Hall Thruster Variants, *Physics of plasmas*, Vol. 8, 11,2001, pp. 5025-5033.
3 Kim, V., "Main physical feature and processes determining the performance of stationary plasma thrusters," *journal of Propulsion and Power*, Vol. 14, .5, 1998, pp. 736-743.
4 Morozov, A. I., Esipchuk, Yu. V., Tilinin, G. N., Trofimov, A. V., Sharov, Yu. A., Shchepkin, G. Ya., " Plasma Accelerator with Closed Electron Drift and Extended Acceleration Zone," *Soviet Physics-Technical Physics*, Vol. 17, 1, July, 1972   pp. 38-45.
5 Zharinov, A. V. and Popov, Yu. S., "Acceleration of Plasma by a Closed Hall current," *Soviet Physics-Technical Physics*, Vol. 12, 1967, pp. 208-211.
6 Semenkin, A., "Investigation of Erosion in Anode Layer Thrusters and Elaboration High Life Design Scheme," IEPC Paper 93-231, Sept. 1993.
7 Popov Yu. S. and Zolotaikin Yu M. "Effect of Anomalous Conductivity on the Structure of the anode Sheath in a Hall Current ion source" *Soviet journal of Plasma Physics*, Vol. 3, No.2 March-April   1977 pp. 210-213
8 Zhurin, V. V. Kaufman, H. R. Robinson, R. S. : Physics of Closed Drift Thrusters, *Plasma sources science & technology*, 8, 1999, R1-R20
9 Baranov, V. I., Nazarenko, Yu. S., Petrosov, V. A., Vasin, A. I., and Yashonov, Yu. M. "Theory of oscillations and Conductivity For Hall Thruster," AIAA Paper 96-3192, July 1996
10 Fife, J. M., Martinez-Sanchez, M., and Szabo, James, "A numerical study of low-frequency discharge oscillations in Hall thrusters," AIAA Paper 97-3052, July 1997.
11 Boeuf, J.P.   and Garrigues, L. "Low Frequency Oscillation in a Stationary Plasma Thruster," *Journal of Applied Physics* , Vol. 84, 7, 1998, pp. 3541-3554.
12 Sasoh, A., Arakawa, Y.: A high resolution thrust stand for ground tests of low-thrust space propulsion devices, *Review of Scientific instruments*, Vol. 64, 3, March 1993, pp. 719-723.
13 Komurasaki, K. and Kusamoto, D., "Optical Measurement o Plasma Oscillations in a Hall Thruster" *Transactions of the Japan Society for Aeronautical and Space Sciences*, Vol. 42, 134, 1999 pp. 203-208.
14 Baranov, V. I., Nazarenko, Yu. S., Petrosov, V. A., Vasin, A. I., and Yashonov, Yu. M. "The Ionization Oscillations Mechanism in ACD," IEPC Paper 95-059, Sept., 1995
15 Yamamoto N., Komurasaki K. and Arakawa Y. "control of Discharge Current Oscillation in Hall Thrusters " International Symposium on Space Technology and Science paper 2004-b32, June 2004.
16 Komurasaki, K., Arakawa, Y: Hall-Current Ion Thruster Performance, *journal of Propulsion and Power*, Vol. **8**, .6, 1992, pp. 1212-1216.
17 Yamamoto N., Komurasaki K. and Arakawa Y. "Condition of Stable Operation in a Hall Thruster " IEPC paper 03-086, Mar., 2003